

# A Classification Method for Myoelectric Control of Hand Prostheses Inspired by Muscle Coordination

Gauravkumar K. Patel, Claudio Castellini, *Member, IEEE*, Janne M. Hahne, Dario Farina, *Senior Member, IEEE*, and Strahinja Dosen, *Member, IEEE*

**Abstract**—Dexterous upper-limb myoelectric prostheses can, to some extent, restore the motor functions lost after an amputation. However, ensuring the reliability of myoelectric control is still an open challenge. In this study, we propose a classification method that exploits the regularity in muscle activation patterns (uniform scaling) across different force levels within a given movement class. This assumption leads to a simple training procedure, using training data collected at single contraction intensity for each movement class. The proposed method was compared to the widely accepted benchmark (LDA classifier) using offline and online evaluation. The offline classification errors obtained with the new method were either lower or higher than LDA depending upon the chosen feature set. In the online evaluation, the new classification method was operated using amplitude-EMG features and compared to the state-of-the-art LDA classifier combined with the time domain feature set. The online evaluation was performed in 11 able-bodied and an amputee subject using a set of four functional tasks mimicking daily-life activities. The tasks assessed the dexterity (e.g. switching between functions) and robustness of control (e.g. handling heavy objects). With the new classification scheme, the amputee performed better in all functional tasks whereas the able-bodied subjects performed significantly better in three out of four functional tasks. Overall, the novel method outperformed the state-of-the-art approach (LDA) while utilizing less training data and a smaller feature set. The proposed method is, therefore, a simple but effective and robust classification scheme, convenient for online implementation and clinical use.

**Index Terms**—Myoelectric control, cosine similarity, fast training, functional tasks, muscle coordination, hand prosthesis.

The work has been supported by the German Ministry for Education and Research (BMBF) under the project INOPRO (16SV7657) and by the EU project INPUT (H2020-ICT-2015-687795). (Corresponding author: Strahinja Dosen.)

G. K. Patel and J. M. Hahne are with the Applied Surgical and Rehabilitation Technology Lab, Department of Trauma Surgery, Orthopedics and Plastic Surgery, University Medical Center Göttingen, 37075 Göttingen, Germany (email: gauravkumar.patel@bccn.uni-goettingen.de, janne.hahne@med.uni-goettingen.de).

C. Castellini is with the Institute of Robotics and Mechatronics, DLR - German Aerospace Center, D-82234 Wessling, Germany (email: claudio.castellini@dlr.de).

D. Farina is with the Department of Bioengineering, Imperial College London, London, UK (email: d.farina@imperial.ac.uk).

S. Dosen is with the Faculty of Medicine, Department of Health Science and Technology, Center for Sensory-Motor Interaction, Fredrik Bajers Vej 7, DK-9220 Aalborg, Denmark (email: sdosen@hst.aau.dk).

## I. INTRODUCTION

Our arms are required to accomplish most daily living activities and therefore, the loss of upper limbs, total or partial, leads to severe impairments. Today, it is possible to replace a missing limb with a dexterous prosthesis, but the available human-machine-interfaces (HMIs) connecting the user and the device lack reliability and intuitive control. While the mechanical design of available dexterous prosthetic hands/arms is sufficiently advanced, the HMI connecting the patient and the prosthesis is a critical bottleneck. Consequently, the rejection rates for myoelectric prostheses are still high, about one third for pediatric and one fourth for adult patients [1].

Most active prostheses are controlled by surface electromyography (sEMG) signals, capturing the user's muscle activity. The classic two-channel sequential and proportional control utilizes EMG signals from two antagonistic muscles to control a single degree-of-freedom (DoF) at a time and muscle co-activation for switching between DoFs [2]. This scheme is slow and non-intuitive. To overcome these limitations, several EMG classification methods have been proposed with promising results [3]–[7]. With classification-based control, the user can activate the desired prosthesis function directly by producing a muscle pattern that was associated with that function during supervised training.

The classification schemes used for myoelectric control follow the conventional pattern-recognition paradigm. The training data is collected using a supervised procedure, and a classification function is fitted over the collected data. During online control, the trained classifier is used to map the user-generated EMG activations to control commands for the prosthesis. This approach has produced encouraging results in laboratory conditions, but so far its translation into clinical systems is rather limited [8], [9]. Nevertheless, there are some commercially available systems (such as the Complete Control system by COAPT [10]) implementing a control based on pattern recognition, but they are yet to prevail in clinical practices. In essence, a truly multifunctional prosthetic limb with natural control over all degrees of freedom is yet to be realized [11].

An important shortcoming of the conventional approach is that it does not exploit the knowledge of physiological phenomenon responsible for the observable muscle activation. Rather, a set of numerical features are computed from the

collected signals and used to train the classifier, which is then expected to implicitly capture the regularity and patterns in the underlying data. However, this generalization may often fail. For example, the information on how some forearm muscles may act consistently in a coordinated manner cannot be explicitly modelled by commonly applied classification algorithms, such as the Linear Discriminant Analysis (LDA) [12]. In this paper, we propose a novel classification method that utilizes the knowledge of muscle coordination to classify hand movements. We then demonstrate that the presented method leads to a more robust and reliable performance during functional tasks.

In literature, the phenomenon of muscle coordination has been previously observed for both intrinsic and extrinsic finger movements [13], [14]. These studies have demonstrated that force production for a given movement relies on the coordination of different muscles and the EMG amplitude of active muscles scales uniformly as a function of applied force during muscle contraction. In [13], the subjects modulated fingertip forces while the EMG was recorded from all muscles of the forefinger. The study has shown that muscle activation patterns (MAPs), represented by a vector of EMG amplitudes recorded from different muscles, were highly correlated across different force levels of a given movement. Therefore, the same set of muscles produced the movement with the same relative amplitude between the muscles. It was later demonstrated in [14] that a similar result holds for a multi-digit grasp. In this case, the MAP included 12 intrinsic and extrinsic finger muscles and the vectors scaled uniformly across the force levels, as assessed by the cosine of the angle between the respective MAPs. From a neuroscientific perspective, muscle coordination is considered habitual [15], i.e. the brain associates each movement to a particular muscle activation pattern which is (habitually) reproduced each time the movement is performed. Furthermore, new activation patterns can be elicited and exercised, for instance by asking users to perform abstract movements (or task) using arbitrary muscles [16]; however, the rate of learning might vary depending on the selected muscles [17]. Such physiological properties associated with muscle coordination could be exploited to improve myoelectric control for the upper-limb prosthesis. In the present study, we focus on one specific property, i.e. the consistent recruitment and activation scaling of the same muscles for a given natural movement, and we show how this can be exploited to establish natural class boundaries in the feature space for myoelectric classification.

The aforementioned motor control studies have already been used as an inspiration for improving pattern-recognition control [18], [19]. However, [18] and [19] did not exploit the intrinsic regularity present directly in the amplitude-related EMG features; instead, they proposed new methods for feature extraction. For example, [18] proposed a novel feature extraction scheme based on the discrete Fourier transform to produce EMG features invariant against muscle contraction levels. Recently, [19] presented a scheme to minimize the effect of force variation on the performance of pattern classification, wherein the feature-set used for classification

was derived by estimating the orientation between the power spectrum of the original EMG signal and its non-linear transformation [19]. In both [18] and [19], the computed force-invariant feature set was presented as input to traditional classifiers (e.g. LDA). It was shown that, when the contraction intensity levels of the training and test data were different (i.e., training on one force level and testing on the other), the classification error for the proposed invariant features was lower than the error observed with classic EMG features (e.g. time-domain features). However, these studies were not evaluated using clinically relevant function tasks, and the analysis was performed using offline data [18], [19].

In the present study, instead of defining new features, we adapt the classification metric to capture the regularities in the feature distribution imposed by muscle coordination. Specifically, we propose to use the standard amplitude-related EMG features in combination with a classification metric that captures the property of muscle coordination. The presented classification method utilizes the well-known cosine similarity metric, which was also applied previously to analyze muscle coordination [13], [14], [18], but has not been used explicitly for classification. The result is a simple and compact method that requires minimal training data and processing. The proposed method is extensively compared with the commonly accepted benchmark (LDA) using both offline and online evaluation. It was hypothesized that using the cosine metric to implement myoelectric classification will establish natural class boundaries in the feature space, and therefore lead to a more reliable control during functional tasks. And indeed, the results demonstrated that despite using fewer features and training data, the proposed method outperforms the benchmark under dynamic conditions of prosthesis use.

The new classification method is explained in Section II, which also discusses data collection for offline analysis and online functional tasks used to evaluate the method. The results for the offline and online evaluation are reported in Section III, and Section IV concludes the work with a summary and general discussion.

## II. MATERIALS AND METHODS

### A. Classification Based on Cosine Similarity

The amplitude of the surface EMG recorded from  $d$  sensors placed around the forearm can be represented using a  $d$ -dimensional MAP vector  $\vec{X} = (MAV_1, MAV_2, \dots, MAV_d)$ , where  $MAV_i$  is the mean absolute value of the  $i^{th}$  EMG channel computed over a time window.

The assumption here is that the EMG signals acquired from forearm muscles scale uniformly in amplitude with contraction intensity [13], [14]. Therefore, the MAP vectors for a given movement point in the same direction, irrespective of the contraction intensity. In practice, the MAP vectors representing different force levels for the same movement will exhibit a distribution that can be modeled as a (hyper-) cone radiating from the origin of the coordinate system. Thus, each movement can be represented using a single prototype MAP vector and the classification can be achieved by measuring the

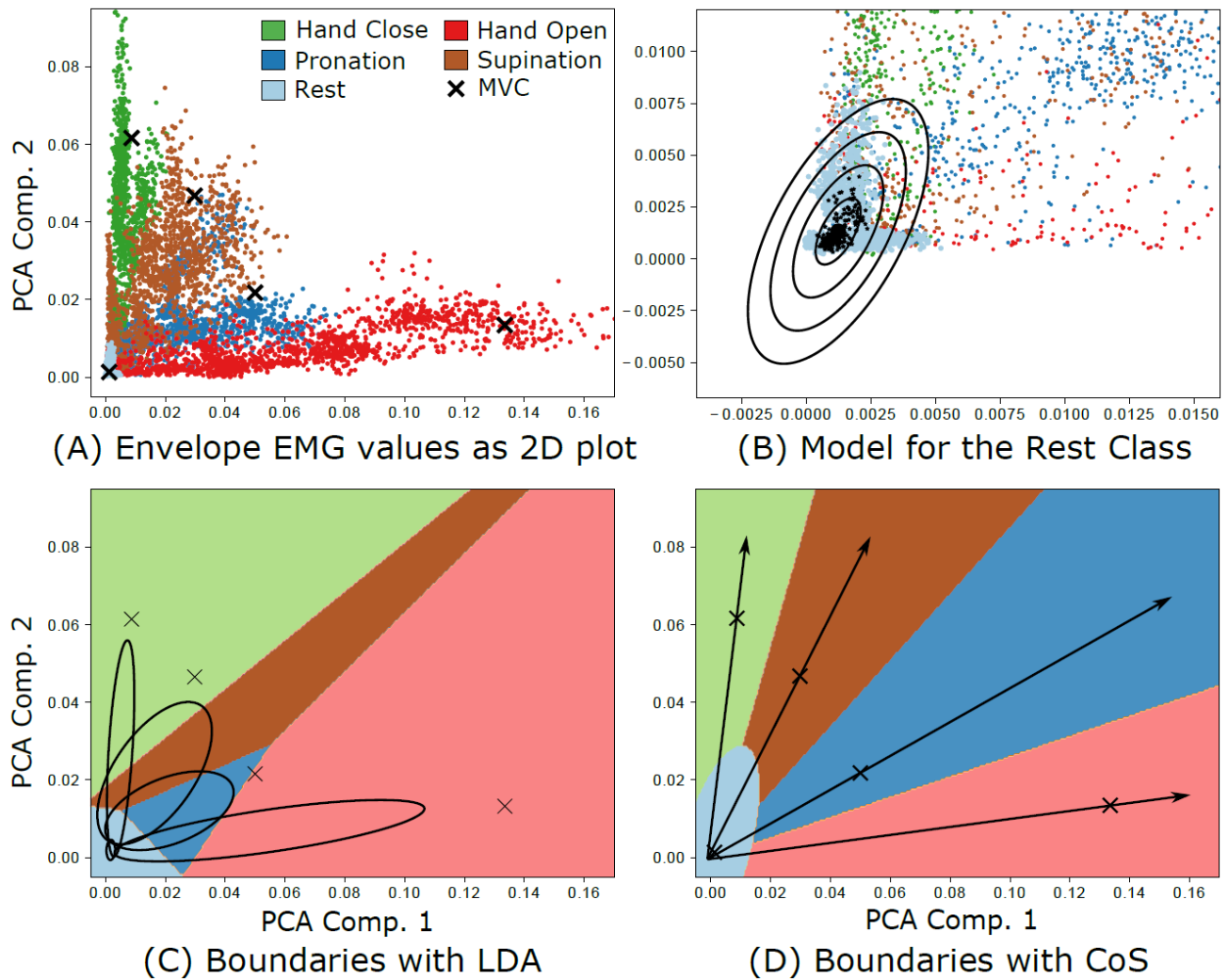


Fig. 1. Proposed method (CoS) vs. classic (LDA) approach. (A) 2D visualization of the training data generated from an able-bodied subject for four different contractions, namely, wrist flexion (Hand Close) and extension (Hand Open), ulnar- and radial-deviations (Pronation and Supination), plus rest. (B) The rest data modelled as a Gaussian distribution. Black points indicate the rest data collected to train the Rest class for the CoS classifier. The visualized Gaussian distribution (black lines) was fitted using only the rest data (black points). Plots (C) and (D) depict the classification boundaries with LDA and CoS trained using the transformed training data. Principal Component Analysis (PCA) was used to reduce the dimensions of the recorded muscle activation patterns (MAPs) from 8 to 2. The explained variance was 81%.

orientation with respect to the registered prototype.

As only the orientation of the prototype vector is required for classification, it becomes possible to evaluate these prototype vectors using training data collected at single contraction intensity. During online control in the present study, the prototype vector for a given movement class was determined by averaging the MAP vectors recorded while performing the movement-specific maximum voluntary contractions (MVC) for 3 seconds. In the classification step, the cosine similarity metric was used to compare an input test-vector with the prototype vector for each movement class. The class that resulted with the maximum cosine similarity was given as the classification output:

$$\operatorname{argmax}_{p \in S_{mov}} \left( \frac{\vec{x} \cdot \vec{v}_p}{\|\vec{x}\| \cdot \|\vec{v}_p\|} \right) \quad (1)$$

where  $\vec{x}$  is an input MAP vector containing amplitude-related EMG values from  $d$  sensors placed on the user,  $\vec{v}_p$  is the

prototype vector for class  $p$ , and  $S_{mov}$  is the set of all movement classes.

The above model can be applied to all classes except for the rest class because the EMG activity for the hand at rest is characterized by low-level noisy activations around some mean value close to the origin of the feature space [20]. Thus, we represented the rest class using a Gaussian distribution with a fixed mean and covariance (Fig. 1B). In the classification step, the distance between an input test-vector  $\vec{x}$  and the mean of the Gaussian distribution was measured using the Mahanobis distance  $d_{MH}(\vec{x})$  as follows:

$$d_{MH}(\vec{x}) = \sqrt{(\vec{x} - \vec{\mu})^T C^{-1} (\vec{x} - \vec{\mu})} \quad (2)$$

where  $\vec{\mu}$  is the mean and  $C$  is the covariance of the rest class. The input MAP vector  $\vec{x}$  was classified as rest if the measured distance  $d_{MH}(\vec{x})$  was less than or equal to a pre-defined

threshold  $T$ , else the vector  $\vec{X}$  was classified according to equation (1) (when  $d_{MH}(\vec{X}) > T$ ). For the online evaluation in the present study, the threshold  $T$  was determined by measuring the Mahalanobis distance  $d_{MH}(\vec{Y})$  for the MVC prototype of the nearest pattern  $\vec{Y}_{nearest}$  and setting the value of  $T$  to 30% of  $d_{MH}(\vec{Y}_{nearest})$ . Hereafter, the proposed classification scheme described above and based on the cosine similarity measure will be abbreviated as CoS.

In summary, the presented classification method selects a distance measure that models the natural distribution of the features in the feature space, i.e. a measure which reflects the coordination of muscle activation across different contraction levels. The method can also be regarded as a simple nearest neighbor classification using class prototypes and cosine similarity as the distance measure.

The difference between the proposed CoS method and the conventional purely data-driven approach (such as LDA) is illustrated in Fig. 1C, D. For didactic purposes, the figure shows classification in a 2D space of projected features (PCA), whereas the method assessment in the present study was conducted using full dimensionality (see next section). An LDA will minimize the model fitting error without considering the physiological relevance of training points. For example, in the depicted case (Fig. 1C), the MVC of “pronation” class is actually assigned to the “hand open” state. As there are no additional constraints apart from minimizing the fitting error on the recorded data, the area of the feature space assigned to the “pronation” class is closed (blue triangle) and rather small compared to other classes. With increasing contraction intensity, the “pronation” vector radiates from the origin and crosses the class boundary. Conversely, the CoS classifier generates physiologically meaningful class boundaries that divide the feature space into open cones, preventing the aforementioned anomaly (Fig. 1D). The proposed method therefore correctly models the data at different contraction intensities. Importantly, this discussion holds for the features that are related to the EMG amplitude comprising the MAP vectors, whereas the features related to the frequency of the signal (e.g., zero crossings) that do not scale with the intensity of contraction [21], might exhibit different distribution patterns.

### B. Signal Acquisition and Processing

The experimental setup comprised eight commercially available double differential EMG electrodes (13E200 AC from Otto Bock, Vienna) placed circumferentially and equidistantly around the forearm, 5 cm distal from the elbow joint, avoiding the area directly above the ulnar bone. In healthy subjects, the electrodes were strapped using an adjustable Velcro band (Fig. 2(A)), whereas a custom-made housing with the electrodes integrated into the socket was used for the amputee subject (Fig. 2(B)). The captured EMG signals were pre-amplified and band-pass filtered by the electrodes and then sampled at 1 kHz using a wireless data acquisition card (AXON Master 10-bit A/D converter, OttoBock, Vienna). The EMG data were transferred to a desktop

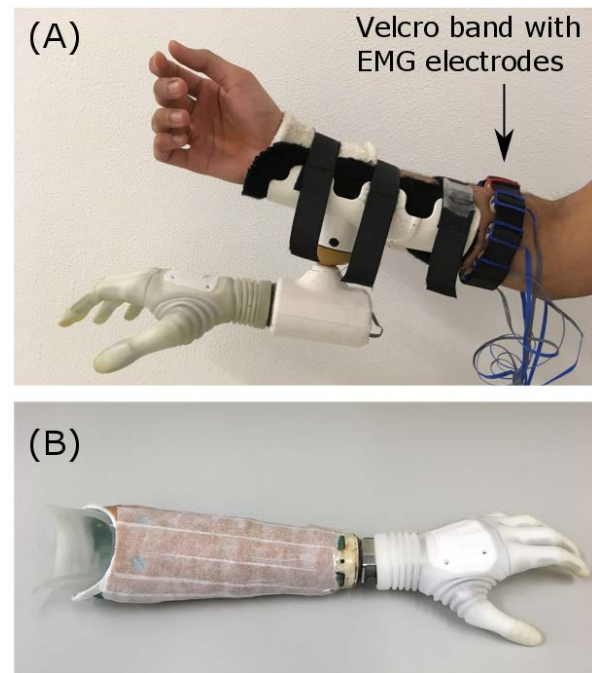


Fig. 2. (A) The custom-made bypass socket used for able-bodied subjects. (B) The custom-made prosthesis socket used by the amputee subject.

computer using a Bluetooth connection, where it was further processed by our software framework. The most commonly used Hudgins time domain features were evaluated for each EMG channel, by segmenting the raw EMG data using intervals of 128 ms and an increment of 32 ms per frame [22], [23]. The acquired EMG data was either stored for offline analysis or used for real-time prosthesis control. The experimental protocols used for offline and real-time evaluations are discussed below. All presented experimental evaluations were approved by the local ethics committee at the University of Göttingen and were conducted according to the declaration of Helsinki. All participating subjects signed an informed consent form.

### C. Offline Evaluation

The data for offline evaluation was collected from seven able-bodied subjects (age range 19-30 yrs.). The subjects stood in front of a computer screen with their elbows flexed at 90°. The EMG data were recorded by performing non-isometric contraction of eight movement classes namely, wrist flexion and extension, pronation and supination, ulnar- and radial-deviation, and hand close and open. First, the MVC of each class was produced for 3 seconds and used as a reference for measuring the normalized strength of each movement. Thereafter, for each movement, the subjects were asked to track trapezoidal trajectories with plateaus normalized to 40% (*Lev1*) and 80% (*Lev2*) of MVC. The subjects performed the tracking using a cursor indicating the strength of the corresponding movement. The vertical position of the cursor was calculated by removing the mean baseline EMG and then normalizing the sum of EMG amplitude values by the sum of MVC amplitudes of the respective movement. The duration of each trajectory was 9 s (2-s rise, 5-s hold, 2-s fall time), followed by a 2-s rest interval between the trajectories (and if

needed, the subject could explicitly ask for an extended rest interval). In total, the subjects repeated each movement and level four times. The first two repetitions were used as training data for classifiers (CoS and LDA) and the last two repetitions were used for testing the classification performance. The CoS classifier was trained using MAV features only (CoS+MAV), whereas the LDA classifier was trained using either MAV features only (LDA+MAV) or the full time-domain feature set (LDA+TD). The three classification schemes (namely, CoS+MAV, LDA+MAV, LDA+TD) were tested under three different offline evaluation scenarios: 1) *Overall* evaluation: where the classifiers were trained using Lev1 and Lev2 data and then tested on both levels. Here, for the CoS classifier, the prototype vector of each movement was calculated by averaging data from both levels. 2) *Lev1\_vs\_Lev2* evaluation: where the classifiers were trained using Lev1 data and then tested for Lev2 data, and 3) *Lev2\_vs\_Lev1* evaluation: where the classifiers were trained using Lev2 data and then tested using Lev1 data. Importantly, the CoS classifier normally does not need to be trained using data from different force levels, as explained previously. This has been done only in the offline analysis for the sake of completeness.

#### D. Online Evaluation

Eleven able-bodied subjects (age range 20-39 yrs.) and one male transradial amputee subject participated in the online experiment. The amputee was 57 years old and his left hand was amputated approximately 36 years ago due to a traumatic injury. As shown in Fig. 2, the able-bodied subjects were fitted with a bypass socket attached to a right-handed Michelangelo prosthesis (Otto Bock, Vienna) and the amputee was fitted with a custom-made socket attached to a left-handed Michelangelo prosthesis. For the real-time evaluation, the LDA classifier was trained following the methods suggested in [22]–[24], whereas the CoS classifier was implemented by using the MVC of each movement as the prototype vector for classification. Both classifiers were used for the sequential and proportional control of four prosthesis functions, namely, palmar grip closing, hand opening, wrist pronation and supination. For the able-bodied subjects, these prosthesis functions were mapped to four contraction patterns, namely, wrist flexion, wrist extension, ulnar- and radial-deviation respectively. For the amputee, a spider plot was employed to judge which muscle contraction patterns could be used for online control. This was done by asking the amputee to generate different patterns on the spider plot (by imagining different movements), and then the four patterns with the most distinct shape were taken. In the end, the flexion, fingers stretched, pronation and supination patterns were used for the control.

The training for the CoS classifier was simple and brief. The subjects only needed to produce the MVC of four classification patterns and the relaxed-hand state for the rest class, each for 3 seconds. Recording data at different force levels [21], [25] and arm postures [26], [27] is recommended for LDA, and therefore, each LDA class was trained at three force levels and three arm postures [23]. To collect the training data, the subjects were asked to track trapezoidal trajectories, with plateaus normalized to 30%, 60% and 90% of MVC. The subjects performed the tracking by using a

cursor indicating the sum of amplitude values across all electrodes normalized by the sum of class MVC values. The duration of each trajectory was 5 s (1-s rise, 3-s hold, 1-s fall time), followed by a 2-s rest interval between the trajectories (and if needed, the subject could explicitly ask for an extended rest interval). In total, 15 movement trajectories were presented in one run and three runs were recorded in three arm postures, namely, elbow flexed in front of the torso, arm relaxed next to the body and arm stretched forward in the sagittal plane at the shoulder level [23]. The recording of the training data took approximately 30 s for CoS and about 7 minutes for the LDA. Moreover, the full time-domain feature set was used to train and control the LDA, whereas the CoS operated using only the MAV features. In the post-processing step for both LDA and CoS, a majority vote of seven samples was applied to the classification stream [22], [23]. The strength of the classified movement was determined by removing the mean baseline EMG activity and then normalizing the sum of input amplitude values by the sum of MVC amplitudes of the detected movement class. Thereafter, the desired normalized velocity of the prosthesis motor (i.e., 0 – no movement, 1 – maximum velocity) was determined by applying a fixed threshold of 0.2 and a gain of 1.2 to the estimated strength of the detected movement. Finally, the estimated velocity was transmitted wirelessly (using Bluetooth) to control the required prosthesis function.

Before starting the experiment, the subjects were introduced to the concept of myoelectric control and fitted with the prosthetic hand. Then, the training data for classification was collected as mentioned above. The performance of the CoS classifier was compared to that of the LDA classifier using a set of four functional tasks (as described in section II.E). The subjects received instructions on how each task had to be completed, and they were asked to practice each task at least once, in order to familiarize with the setup and the protocol. The real-time assessment was divided into two evaluation segments, and in each segment, a different control method (either LDA or CoS) was administered randomly, i.e., half subjects used LDA before CoS and vice versa. In a given evaluation segment, the subjects sequentially performed four rounds of the Box-and-Blocks, Clothespin, Bottle Transfer and Bottle Turn task, i.e. they performed four rounds of Box-and-Blocks task followed by four rounds of Clothespin test and so on.

After the experiment, the subjects reported their subjective experience of the two control methods. Each method was subjectively scored with a number between 0 and 10; where 10 represented the best control over all prosthetic movements. In the beginning, the subjects were informed that the experiment was designed to compare two control methods, but in order to avoid any expectation bias, the order and the exact details of the methods (LDA or CoS) were not disclosed.

#### E. Online Tests

The online control was evaluated using four functional tasks with a varying level of difficulty. In each task, the subject performed four rounds (as described below) using each of the two control methods (LDA and CoS).

**Box-and-blocks test:** This is a commonly used standardized functional test for evaluating the performance of

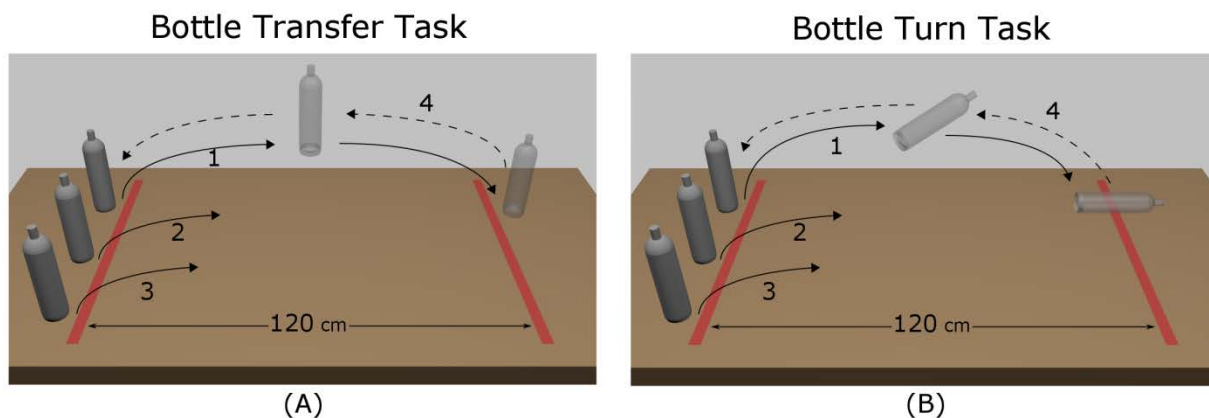


Fig. 3. (A) The bottle transfer task. Three bottles, initially placed on the side where the subject wore the prosthesis (here left), must be transferred one-by-one from the left side of the table to the right side and then back to their initial position. (B) The bottle turn task. From left to right, each bottle must be turned over, then laid down horizontally and vice-versa (from right to left).

myoelectric control, specifically, the ability to grasp and transfer a rigid object [28]. In a single round, the subjects were asked to transfer as many blocks as possible, from one compartment to the other, within 60 seconds. The test required only the opening and closing of the prosthesis, i.e. only a single degree of freedom (DoF) was utilized. The outcome measure was the number of blocks transferred.

**Clothespin test:** In a single round, the subjects were asked to pick up three pins from a horizontal bar, rotate them and place them on a vertical bar. This test required a dexterous control over 2-DoFs, i.e. switching between opening/closing and pronation/supination. The outcome measure was the time required to successfully transfer three pins. The Rolyan Graded Pinch Exerciser [29] was used in this experiment, with three red pins requiring about 10 N of gripping force.

**Bottle transfer task:** This (and the following) task was designed to evaluate the robustness of control when transferring and manipulating heavy objects. As shown in Fig. 3(A), two parallel lines with 120 cm distance were marked on the surface of a table with length 2 m, width 80 cm, and height 80 cm. The floor in front of the table was marked with a 60 cm square, and the subjects were instructed not to step out from the square during the task. Three water-bottles (diameter 6 cm and height 25 cm) filled with 1 L of water (approx. 1 kg) were placed on the table, aligned along the line on the side of the prosthesis. In a single round, the subject had to pick up the three bottles, one at a time, and transfer them to the other side of the table. Next, the subjects had to transfer the same three bottles back to their initial position, thereby completing a single round. The task sequence is outlined in Fig. 3(A). If a bottle was dropped during lift/transfer/placement, it was placed back to its initial position by the subject using the able hand and the transfer was restarted. The two outcome measures evaluated for this task were the round completion time and the number of bottles dropped per round.

**Bottle turn task:** The setup was the same as in the previous task. The subjects had to pick up a bottle, turn it by about 90° to horizontal orientation and then lay it down on the other side. This was done one-by-one for all three bottles. Next, the bottles were picked up, turned to vertical orientation

and placed back to their initial position, thereby completing a single round. If the subject dropped a bottle, the transfer was restarted, as in the previous task. This task required manipulating heavy objects using 2 prosthesis DoFs. The round completion time and the number of bottles dropped per round were evaluated as outcome measures.

#### F. Statistical Evaluation

Each outcome measure was tested for normality and depending on the outcome of the test, either a paired t-test or a Wilcoxon signed rank test was used to compare the performance of LDA versus CoS. All results are reported as mean  $\pm$  standard deviation and the threshold for significance was set to  $p < 0.05$ .

### III. RESULTS

#### A. Offline Evaluation

The summary results for the offline evaluation are shown in Fig. 4. The classification error for the *Overall* evaluation with CoS+MAV (17.5 $\pm$ 10.4%) was significantly lower than LDA+MAV (21.3 $\pm$ 10.6%), but significantly higher compared to LDA+TD (10.8 $\pm$ 6.1%). In the *Lev1\_vs\_Lev2* evaluation, the LDA+TD (13.8 $\pm$ 6.7%) performed significantly better than both LDA+MAV (22.8 $\pm$ 12.3%) and CoS+MAV (23.7 $\pm$ 12.8%), which performed similarly. Finally, the classification error with CoS+MAV (21.4 $\pm$ 14.1%) in the *Lev2\_vs\_Lev1* evaluation was significantly lower than LDA+MAV (33.6 $\pm$ 12.3%) but significantly higher than LDA+TD (16 $\pm$ 9.5%). Thus, the LDA+TD consistently outperformed the LDA+MAV or CoS+MAV in all three offline evaluations, whereas the CoS+MAV was either better than or similar to LDA+MAV. In most cases, the classification accuracy decreased significantly when the methods were trained on one force level and tested on another, which is a well-established result [18], [19], [25]. This observation did not hold only for LDA+MAV wherein the *Overall* and *Lev1\_vs\_Lev2* errors were statistically similar.

The confusion matrices for the *Overall* evaluation were examined to understand which movements were most problematic for the three methods. The confusion matrix for

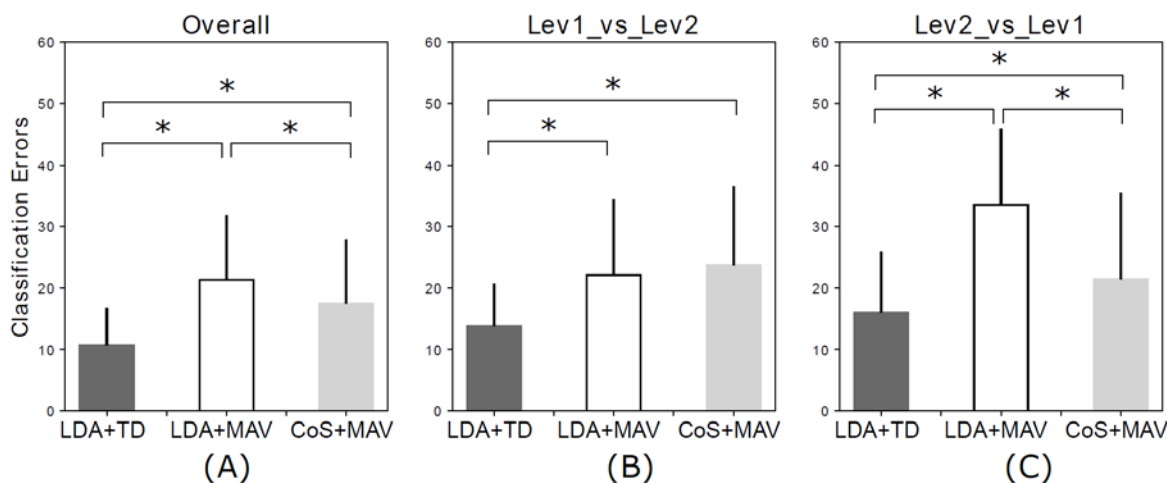


Fig. 4. Summary results (mean  $\pm$  standard deviation) for the offline analysis in able-bodied subjects. The LDA classifier combined with the time domain (TD) features always performed better than LDA or CoS classifier using only mean absolute value (MAV) features. Next, CoS+MAV performed better than LDA+MAV for the *Overall* (A) and *Lev2\_vs\_Lev1* (C) analysis and the performance was similar to LDA+MAV for the *Lev1\_vs\_Lev2* (B) analysis.

CoS+MAV showed that flexion, extension and hand close resulted in the classification accuracy greater than 90%, while the accuracy for radial-deviation, pronation and supination was approximately 80%. The accuracy for the hand open and ulnar deviation was less than 80%. Here, hand open was often misclassified as pronation, and ulnar deviation was often misclassified as supination or hand close. Next, the confusion matrix for LDA+TD showed that flexion, hand close, radial-deviation, and supination were classified with the accuracy greater than 90%, while the extension, ulnar deviation, and pronation resulted in the accuracy greater than 80%. The accuracy for the hand open was less than 80% (due to unwanted misclassifications with ulnar/radial-deviation, pronation, and supination). Lastly, the confusion matrix for LDA+MAV revealed that the accuracy for all the classes was below 90%. The classification success rates for the flexion, hand closed, radial-deviation and supination were higher than 80%, and for the extension, ulnar-deviation, pronation and hand open, they were less than 80%.

### B. Online Evaluation

The summary results for the online assessment in able-bodied subjects are shown in Fig. 5. For the box and blocks test, the subjects transferred  $12.4 \pm 3.9$  blocks in one minute using CoS, which was slightly but significantly higher than  $11.5 \pm 3.3$  blocks with LDA. The average time taken to transfer three pins was similar for both CoS and LDA,  $29 \pm 11$  s and  $31 \pm 13$  s, respectively. The subjects were significantly faster with CoS compared to LDA in both bottle transfer ( $40 \pm 14$  s vs.  $51 \pm 25$  s) and bottle turn task ( $59 \pm 25$  s vs.  $73 \pm 27$  s). This corresponds to an average decrease of 22% and 19% in the task completion time with CoS for the bottle transfer and turn tasks, respectively.

The summary results for the online assessment in the amputee subject are shown in Fig. 6. In the box and blocks test, the amputee transferred 41% more blocks with CoS,  $24.8 \pm 0.8$  vs.  $17.5 \pm 1.1$  blocks with LDA. The average time taken to transfer three pins was  $12 \pm 1$  s with CoS and  $16 \pm 1$  s with LDA. The average task completion times for the bottle

transfer and turn tasks were  $21 \pm 2$  s and  $33 \pm 6$  s for CoS versus  $38 \pm 5$  s and  $45 \pm 1$  s for LDA, respectively. Therefore, with CoS, the average task completion time decreased by approximately 25%, 37%, and 16% for the clothespin, bottle transfer and turn tasks, respectively.

The number of bottles dropped during the bottle transfer task with CoS and LDA in able-bodied subjects was similar, i.e.,  $0.18 \pm 0.44$  vs  $0.43 \pm 0.84$  drops per round, respectively (Fig. 7). For the bottle turn task, the number of bottles dropped with CoS ( $0.36 \pm 0.71$ ) was significantly lower than LDA ( $0.89 \pm 1.1$ ) (Fig. 7). The amputee did not drop any bottles during the bottle transfer or turn tasks with neither of the two methods.

The subjective assessment given by the able-bodied subjects was generally in favor of CoS with respect to LDA. Specifically, 8 out of 11 subjects reported better experience with CoS, 2 subjects reported better experience with LDA and 1 subject reported perceiving no difference between LDA and CoS. The amputee gave a subjective score of 8 to CoS and 4 to LDA, i.e. CoS was preferred over LDA. Specifically, the amputee reported having problems when trying to open the hand with LDA, as hand-opening commands were often misclassified as wrist pronation. As shown in Fig. 8, this problem was more dominant while controlling the prosthesis using LDA. Finally, the average subjective score given by all twelve subjects for CoS was significantly higher than the score for LDA,  $7.3 \pm 0.9$  vs  $5.7 \pm 1.6$  ( $p < 0.05$ ).

## IV. DISCUSSION

A myoelectric classification method (CoS) inspired by the physiology of muscle coordination has been introduced and extensively compared to a state-of-the-art classifier (LDA) using offline and online evaluations. The main idea behind the novel method (CoS) was to demonstrate how an insight regarding the regularity in the generation of muscle activation patterns (consistent scaling with forces) can be translated into a simple classification scheme that provides robust performance, as assessed through a set of relevant and

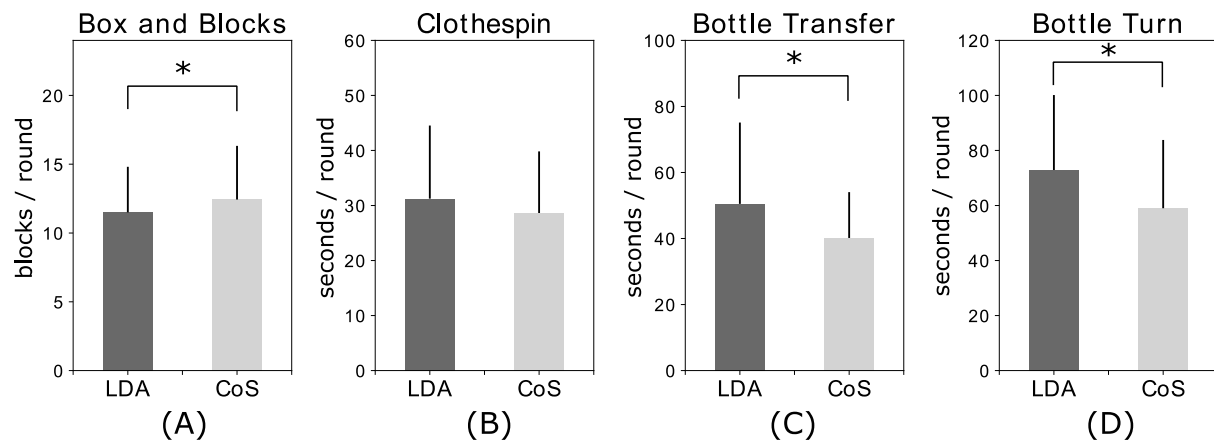


Fig. 5. The summary results (mean  $\pm$  standard deviation) for the online tests in the able-bodied subjects. (A) In the box and blocks test, CoS performed better than LDA. (B) In the clothespin test, no difference in performance between LDA and CoS was observed. In the bottle transfer (C) and turn tasks (D), CoS outperformed LDA. (\* indicates  $p < 0.05$ )

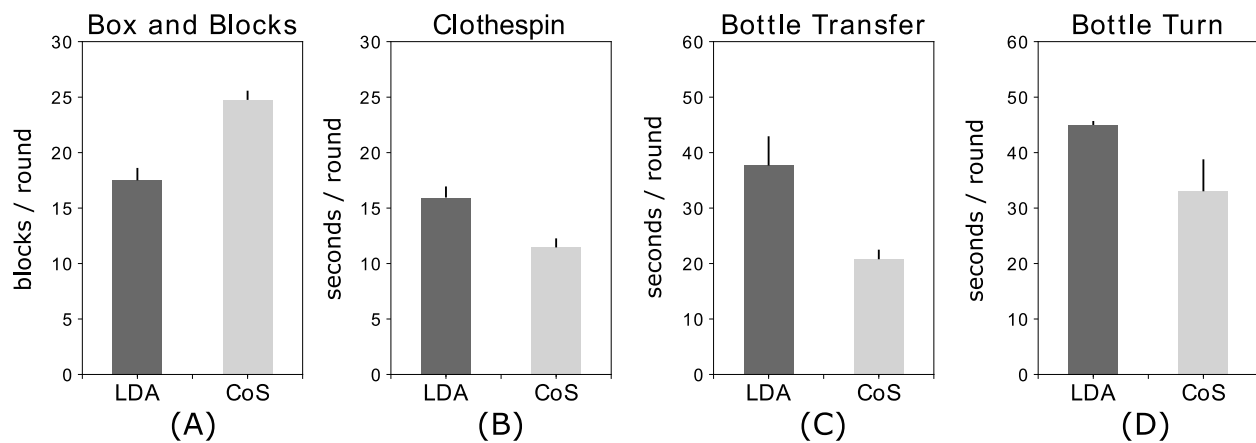


Fig. 6. The results of the online test in the amputee subject: (A) Box and blocks test (B) Clothespin test (C) Bottle transfer test (D) Bottle turn test. The CoS performed better than LDA consistently in all the tasks. Additionally, the amputee reported better user-experience when using CoS for prosthesis control compared to LDA.

challenging functional tests. In general, the study also points to the potential advantage of approaches that are “inspired” by the underlying muscle coordination mechanisms over purely data-driven methods that largely prevail in the literature.

Firstly, the CoS classifier was compared to the LDA classifier using an offline evaluation. The classification errors obtained with CoS were either lower or higher than LDA depending upon the chosen feature set. In particular, the errors with CoS were always higher than the state-of-the-art LDA+TD classifier. This observation is contradictory to the online evaluation and can be seen as a weakness of the offline data analysis. In fact, it has been previously shown that offline results hardly offer an insight regarding the real-time testing effectiveness [32], [33]. Our main assumption, as stated in Introduction, was that the natural classification boundaries imposed by cosine similarity classification would be advantageous in dynamic conditions because such boundaries might allow better generalization when the muscle patterns change during functional use. And indeed, the online tests have supported this hypothesis.

The online evaluation demonstrated that the CoS classifier significantly outperformed the state-of-the-art LDA classifier

in three out of four tasks for the able-bodied subjects and it performed consistently better than LDA in all the tasks for the amputee subject. Additionally, the CoS also offered a number of practical advantages over LDA, including a reduction in the overall training time and the computational cost. The time required to train CoS (30 s) was much lower than LDA (7 min). Further, an 8-dimensional amplitude-related EMG feature space was used for movement classification with CoS, versus a 32-dimensional time-domain feature space used for LDA classification. This reduces the overall computational cost and offers a possibility to simplify the EMG acquisition setup. For example, the EMG signals can be sampled at a lower rate ( $\sim 100$  Hz) to extract amplitude related features as compared to a high sampling rate ( $\sim 1$  kHz) that is necessary to capture full spectral information.

An important aim of the present online experiment was to provide a clinically relevant evaluation of our method. Four essential upper-limb functions (2 DoFs, i.e. closing/opening of the hand and supination/pronation of the wrist) were included in the experimental protocol, as they are considered the most important functions for transradial amputees [34]. This configuration is also common in many commercially available

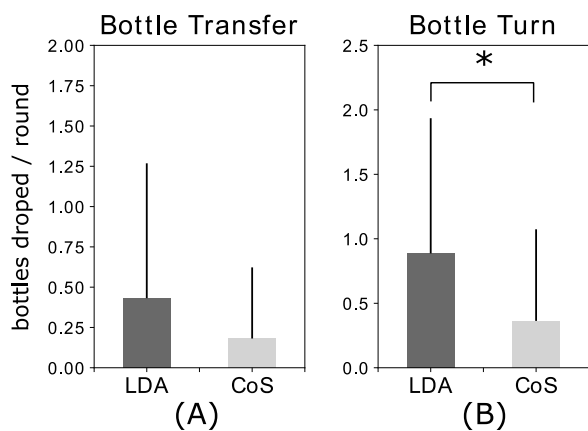


Fig. 7. Number of bottles dropped per round by able-bodied subjects during the bottle transfer (A) and turn (B) tasks, respectively. (\* indicates  $p < 0.05$ )

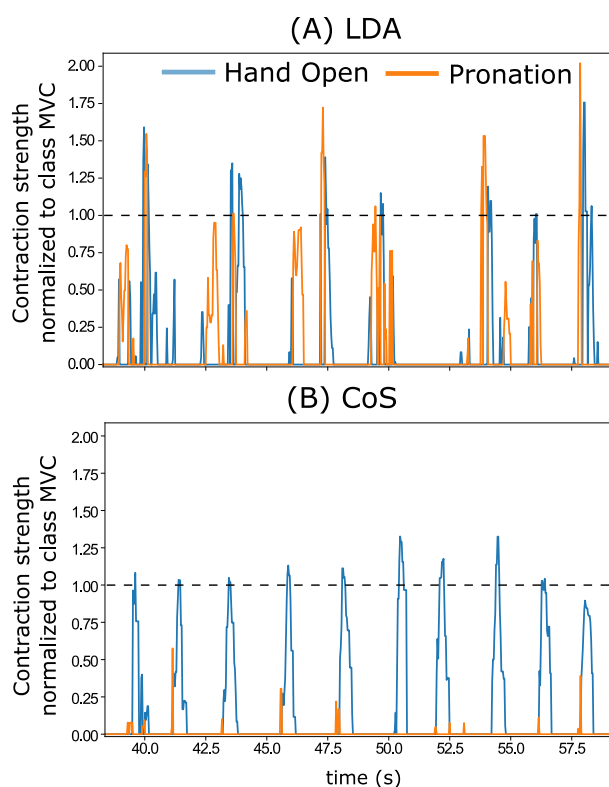


Fig. 8. Prosthesis command signals (hand opening and pronation) estimated during the box and blocks test for the amputee when using LDA (A) and CoS (B) for prosthesis control. Occasionally, the hand opening command was misclassified as pronation by both LDA and CoS. However, the misclassifications were more frequent and stronger when using LDA. (The box and blocks test required only hand opening and closing for task completion, and therefore we assume that the amputee did not intentionally activate pronation during the test.)

hand prostheses (i.e. a gripper with an active wrist), and has been used in some recent clinically relevant studies, investigating sequential [35], [36] and simultaneous [37], [38] myoelectric control. Next, the practical benefits associated with the presented method also make it promising for clinical applications. A prolonged training time can limit the clinical viability of the system [39]. The training required for CoS is

brief and therefore easy to perform whenever the system needs to be recalibrated. The classification formula is simple and reduces to computing a product between few 8-dimensional vectors. This, and the fact that only prototype vectors need to be stored in memory, makes the method suitable for implementation in an embedded system. Furthermore, the method is especially convenient for incremental learning, which is an important mechanism when considering daily-life use [40]. With incremental learning, the prototype for a single class or selected subset of classes, whose classification performance needs to be improved, could be easily updated by recording few additional contractions.

Although a high degree of similarity in orientation between MAP vectors at different intensity levels was observed by [13], [14], [18], a further comparison revealed that MAP vectors with neighboring intensity levels (e.g. 20% vs. 50% and 50% vs. 80%) were still more similar than MAP vectors further apart in intensity levels (e.g. 20% vs. 80%) [18]. Therefore, it has been recommended in [18] and [19] to use training data containing all intensity levels, as it would minimize the effect of dissimilarity in MAP vectors and likely improve the classification accuracy. Nevertheless, the aim of the present study was to emphasize the potential practical benefits arising from the muscle coordination property, specifically, reduction in the training time. Therefore, each movement class was represented using a single prototype MAP vector, i.e. the class MVC.

Many post-processing methods can be used to improve the overall controllability by filtering the output of the classifier. In the present study, we have used majority voting, which is a common choice in the literature [22], [41], [42], but the results may slightly change with another post-processing method (e.g., velocity ramp [43]). However, even if another post-processing scheme could improve the overall controllability, i.e. potentially decreasing the performance gap between CoS and LDA, the presented method is still relevant for clinical use since it has other important advantages, as explained above (i.e. lower training time and smaller computational effort).

The aforementioned motor control studies [13], [14] have been used only as an inspiration for the present work, but our approach has important differences. The studies [13], [14] are related to intrinsic and extrinsic hand muscles while the present experiment also used wrist motions. There are anatomical and physiological differences between intrinsic and extrinsic hand muscles and muscles controlling the wrist [44]–[46], but these differences were not considered while designing the proposed classification method. Rather, we focused on simplifying the experimental settings to suit real-life applications, specifically, by using surface electrodes instead of fine-wire intramuscular electrodes and by placing the electrodes circumferentially around the forearm instead of on specific target muscles. Despite these differences, the results indicate that the recorded muscle activation patterns (MAPs) exhibit the same regularity (distribution along the hypercones) as reported in [13], [14].

Here, we have exploited this regularity of muscle coordination during natural movements (i.e. the regularity of

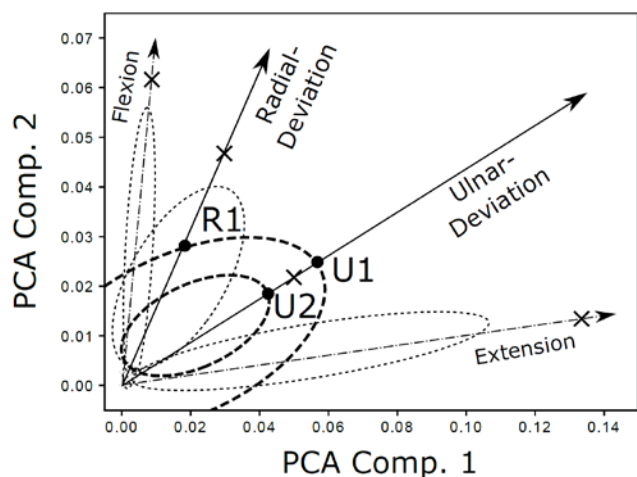


Fig. 11. Comparison of two different modelling approaches to capture the distribution of the EMG features: modelling each class with a Gaussian distribution (as in LDA) versus modelling each class with a line connecting the origin and the MVC, and then using cosine metric (as in CoS). The models were generated from the data shown in Fig. 1(A). The CoS assigns proper likelihoods to the samples (e.g., U1, U2, and R1), and this can be used within the rejection schemes to filter out wrong classification decisions.

MAP distributions) to develop a new classification method. There is an interesting body of work [47]–[50] exploiting the coordinated activation of muscles in a different way, in particular, by applying a linear transformation on the EMG signals acquired from different muscles for controlling a cursor in 2D space. For example, [47] and [48] represented each muscle as a vector acting along uniformly-spaced directions of action, while the position of a 2D cursor was determined by summing up these vectors, whose magnitude was equal to the amplitude of the EMG signal. For online myocontrol, the 2D space was divided into different areas corresponding to various prosthesis functions, e.g. moving the cursor near to the positive x-axis ( $\pm 30^\circ$ ) would activate lateral grip, negative x-axis ( $\pm 30^\circ$ ) would be thumbs up, etc. [49]. The subject then needed to explicitly modulate individual muscle activations using direct control to reach these predefined areas. This kind of control has been patented by the prosthesis manufacturer Touch Bionics (UK) [51]. In the present study, however, instead of asking the subjects to explicitly modulate individual muscles to activate predefined areas in the 2D space, our method allows the subjects to use existing natural movements to activate different areas in the high-dimensional feature space. Importantly, these areas were delimited by physiologically informed boundaries that were captured using the cosine similarity metrics.

Finally, Fig. 9 illustrates an additional comparison between the proposed and the conventional approach to modelling the distribution of EMG features. The points U1 and U2 represent wrist ulnar-deviation with different intensity levels and point R1 represents radial-deviation. From our knowledge of muscle coordination, we expect points U1 and U2 to have the same likelihood (or confidence) of belonging to the ulnar-deviation class and R1 to have a lower likelihood. However, when we model the data using a Gaussian probability distribution, as in LDA, the likelihood assigned to point U1 by the model (Gaussian) associated to the “ulnar-deviation” class is lower

than U2 and, surprisingly, points U1 and R1 have the same likelihood of belonging to the ulnar-deviation class. Conversely, the cosine similarity metric correctly assigns the same level of confidence to points U1 and U2, and a lower confidence for the ulnar-deviation class to point R1. Therefore, the CoS modelling provides a better confidence measure. A good confidence measure can be used to implement a rejection-scheme for filtering-out potentially erroneous classification decisions made by the system. A rejection scheme based on cosine similarity could be used in the future to improve the robustness of control, similar to the rejection schemes based on log-likelihood probabilities for LDA [30], [31].

## V. ACKNOWLEDGEMENT

The graphs and figures presented in the manuscript were created using Inkscape ([www.inkscape.org](http://www.inkscape.org)), Matplotlib with Python 3.3 on the Anaconda framework ([matplotlib.org](http://matplotlib.org), [python.org](http://python.org) and [continuum.io](http://continuum.io)) and Blender ([blender.org](http://blender.org)).

## REFERENCES

- [1] E. Biddiss and T. Chau, “Upper-limb prosthetics: critical factors in device abandonment,” *Am J Phys Med Rehabil*, vol. 86, no. 12, pp. 977–987, 2007.
- [2] P. A. Parker, K. Englehart, and B. Hudgins, “Myoelectric signal processing for control of powered limb prostheses,” *J. Electromyogr. Kinesiol.*, vol. 16, no. 6, 2006.
- [3] Guanglin Li, A. E. Schultz, and T. A. Kuiken, “Quantifying Pattern Recognition—Based Myoelectric Control of Multifunctional Transradial Prostheses,” *IEEE Trans. Neural Syst. Rehabil. Eng.*, vol. 18, no. 2, pp. 185–192, Apr. 2010.
- [4] R. Chowdhury, M. Reaz, M. Ali, A. Bakar, K. Chellappan, and T. Chang, “Surface Electromyography Signal Processing and Classification Techniques,” *Sensors*, vol. 13, no. 9, pp. 12431–12466, Sep. 2013.
- [5] C. Cipriani *et al.*, “Online Myoelectric Control of a Dexterous Hand Prosthesis by Transradial Amputees,” *IEEE Trans. Neural Syst. Rehabil. Eng.*, vol. 19, no. 3, pp. 260–270, Jun. 2011.
- [6] X. Chen, X. Zhu, and D. Zhang, “A discriminant bispectrum feature for surface electromyogram signal classification,” *Med. Eng. Phys.*, vol. 32, no. 2, pp. 126–135, Mar. 2010.
- [7] A. H. Al-Timemy, G. Bugmann, J. Escudero, and N. Outram, “Classification of Finger Movements for the Dexterous Hand Prosthesis Control With Surface Electromyography,” *IEEE J. Biomed. Heal. Informatics*, vol. 17, no. 3, pp. 608–618, May 2013.
- [8] D. Farina and O. Aszmann, “Bionic limbs: clinical reality and academic promises,” *Sci. Transl. Med.*, vol. 6, no. 257, p. 257ps12, Oct. 2014.
- [9] I. Vujaklija *et al.*, “Translating Research on Myoelectric Control into Clinics—Are the Performance Assessment Methods Adequate?,” *Front. Neurobot.*, vol. 11, p. 7, 2017.
- [10] “COAPT Complete Control.” <https://www.coaptengineering.com/>.
- [11] N. Jiang, S. Dosen, K.-R. Müller, and D. Farina, “Myoelectric control of artificial limbs: is there the need for a change of focus?,” *IEEE Signal Process. Mag.*, vol. 29, no. 5, pp. 149–152, 2012.
- [12] G. Rasool, K. Iqbal, N. Bouaynaya, and G. White, “Real-Time Task Discrimination for Myoelectric Control Employing Task-Specific Muscle Synergies,” *IEEE Trans. Neural Syst. Rehabil. Eng.*, vol. 24, no. 1, pp. 98–108, 2016.
- [13] F. J. Valero-Cuevas, “Predictive Modulation of Muscle Coordination Pattern Magnitude Scales Fingertip Force Magnitude Over the Voluntary Range,” *J Neurophysiol*, vol. 83, no. 3, pp. 1469–1479, 2000.
- [14] B. Poston, A. Danna-Dos Santos, M. Jesunathadas, T. M. Hamm, and M. Santello, “Force-Independent Distribution of Correlated Neural Inputs to Hand Muscles During Three-Digit Grasping,” *J. Neurophysiol.*, vol. 104, no. 2, pp. 1141–1154, 2010.

- [15] A. de Rugy, G. E. Loeb, and T. J. Carroll, "Muscle coordination is habitual rather than optimal," *J. Neurosci.*, vol. 32, no. 21, pp. 7384–91, May 2012.
- [16] K. Nazarpour, A. Barnard, and A. Jackson, "Flexible cortical control of task-specific muscle synergies," *J. Neurosci.*, vol. 32, no. 36, pp. 12349–60, Sep. 2012.
- [17] J. Barnes, M. Dyson, and K. Nazarpour Senior Member, "Comparison of Hand and Forearm Muscle Pairs in Controlling of a Novel Myoelectric Interface," *IEEE International Conference on Systems, Man, and Cybernetics (SMC)*, Budapest, 2016, pp. 002846-002849.
- [18] J. He, D. Zhang, X. Sheng, S. Li, and X. Zhu, "Invariant surface EMG feature against varying contraction level for myoelectric control based on muscle coordination," *IEEE J. Biomed. Heal. Informatics*, vol. 19, no. 3, pp. 874–882, 2015.
- [19] A. H. Al-Timemy, R. N. Khushaba, G. Bugmann, and J. Escudero, "Improving the Performance Against Force Variation of EMG Controlled Multifunctional Upper-Limb Prostheses for Transradial Amputees," *IEEE Trans. Neural Syst. Rehabil. Eng.*, vol. 24, no. 6, pp. 650–661, Jun. 2016.
- [20] C. J. De Luca and Z. Erim, "Common drive of motor units in regulation of muscle force," *Trends Neurosci.*, vol. 17, no. 7, pp. 299–305, 1994.
- [21] D. Tkach, H. Huang, and T. A. Kuiken, "Study of stability of time-domain features for electromyographic pattern recognition," *J. Neuroeng. Rehabil.*, vol. 7, no. 1, p. 21, May 2010.
- [22] K. Englehart and B. Hudgins, "A robust, real-time control scheme for multifunction myoelectric control," *IEEE Trans. Biomed. Eng.*, vol. 50, no. 7, pp. 848–854, Jul. 2003.
- [23] S. Amsuess, P. Goebel, B. Graimann, and D. Farina, "A Multi-Class Proportional Myocontrol Algorithm for Upper Limb Prosthesis Control: Validation in Real-Life Scenarios on Amputees," *IEEE Trans. Neural Syst. Rehabil. Eng.*, vol. 23, no. 5, pp. 827–836, Sep. 2015.
- [24] B. Hudgins, P. Parker, and R. N. Scott, "A new strategy for multifunction myoelectric control," *IEEE Trans. Biomed. Eng.*, vol. 40, no. 1, pp. 82–94, 1993.
- [25] E. Scheme and K. Englehart, "Training Strategies for Mitigating the Effect of Proportional Control on Classification in Pattern Recognition Based Myoelectric Control," *J. Prosthet. Orthot.*, vol. 25, no. 2, pp. 76–83, 2013.
- [26] E. Scheme, K. Biron, and K. Englehart, "Improving myoelectric pattern recognition positional robustness using advanced training protocols," in *2011 Annual International Conference of the IEEE Engineering in Medicine and Biology Society*, 2011, pp. 4828–4831.
- [27] Y. Geng *et al.*, "Toward attenuating the impact of arm positions on electromyography pattern-recognition based motion classification in transradial amputees," *J. Neuroeng. Rehabil.*, vol. 9, no. 1, p. 74, 2012.
- [28] V. Mathiowetz, G. Volland, N. Kashman, K. Weber, and K. Mathiowetz, Virgil and Volland, Gloria and Kashman, Nancy and Weber, "Adult norms for the Box and Block Test of manual dexterity," *Am. J. Occup. Ther.*, vol. 39, no. 6, pp. 386–391, 1985.
- [29] "Performance Health." [Online]. Available: <https://www.pattersonmedical.co.uk/>.
- [30] S. Amsuss, P. M. Goebel, Ning Jiang, B. Graimann, L. Paredes, and D. Farina, "Self-Correcting Pattern Recognition System of Surface EMG Signals for Upper Limb Prosthesis Control," *IEEE Trans. Biomed. Eng.*, vol. 61, no. 4, pp. 1167–1176, Apr. 2014.
- [31] E. J. Scheme, B. S. Hudgins, and K. B. Englehart, "Confidence-based rejection for improved pattern recognition myoelectric control," *IEEE Trans. Biomed. Eng.*, vol. 60, no. 6, pp. 1563–1570, 2013.
- [32] M. Ortiz-Catalan, F. Rouhani, R. Branemark, and B. Hakansson, "Offline accuracy: A potentially misleading metric in myoelectric pattern recognition for prosthetic control," in *2015 37th Annual International Conference of the IEEE Engineering in Medicine and Biology Society (EMBC)*, 2015, pp. 1140–1143.
- [33] N. Jiang, I. Vujaklija, H. Rehbaum, B. Graimann, and D. Farina, "Is Accurate Mapping of EMG Signals on Kinematics Needed for Precise Online Myoelectric Control?," *IEEE Trans. Neural Syst. Rehabil. Eng.*, vol. 22, no. 3, pp. 549–558, May 2014.
- [34] W. H. M. Atkins Diane J. OTR; Heard, Denise C Y MSE; Donovan, "Epidemiologic Overview of Individuals with Upper-Limb Loss and Their Reported Research Priorities," *J. Prosthetics Orthot.*, vol. 8, no. 1, pp. 2–11, 1996.
- [35] J. L. Bethausser *et al.*, "Limb Position Tolerant Pattern Recognition for Myoelectric Prosthesis Control with Adaptive Sparse Representations From Extreme Learning," *IEEE Trans. Biomed. Eng.*, vol. 65, no. 4, pp. 770–778, Apr. 2018.
- [36] N. Jiang, T. Lorrain, and D. Farina, "A state-based, proportional myoelectric control method: online validation and comparison with the clinical state-of-the-art," *J. Neuroeng. Rehabil.*, vol. 11, no. 1, p. 110, Jul. 2014.
- [37] J. M. Hahne *et al.*, "Linear and Nonlinear Regression Techniques for Simultaneous and Proportional Myoelectric Control," *IEEE Trans. Neural Syst. Rehabil. Eng.*, vol. 22, no. 2, pp. 269–279, 2014.
- [38] N. Jiang, H. Rehbaum, I. Vujaklija, B. Graimann, and D. Farina, "Intuitive, Online, Simultaneous, and Proportional Myoelectric Control Over Two Degrees-of-Freedom in Upper Limb Amputees," *IEEE Trans. Neural Syst. Rehabil. Eng.*, vol. 22, no. 3, pp. 501–510, May 2014.
- [39] J. W. Sensinger, B. A. Lock, and T. A. Kuiken, "Adaptive Pattern Recognition of Myoelectric Signals: Exploration of Conceptual Framework and Practical Algorithms," *IEEE Trans. Neural Syst. Rehabil. Eng.*, vol. 17, no. 3, pp. 270–278, Jun. 2009.
- [40] C. Castellini, "Incremental learning of muscle synergies: from calibrating a prosthesis to interacting with it," in *Human and robot hands - Sensorimotor Synergies to Bridge the Gap between Neuroscience and Robotics*, A. Moscatelli and M. Bianchi, Eds. Springer Netherlands, 2015.
- [41] R. N. Khushaba, S. Kodagoda, M. Takruri, and G. Dissanayake, "Toward improved control of prosthetic fingers using surface electromyogram (EMG) signals," *Expert Syst. Appl.*, vol. 39, no. 12, pp. 10731–10738, Sep. 2012.
- [42] A. D. C. Chan and K. B. Englehart, "Continuous classification of myoelectric signals for powered prostheses using gaussian mixture models," in *Proceedings of the 25th Annual International Conference of the IEEE Engineering in Medicine and Biology Society (IEEE Cat. No.03CH37439)*, pp. 2841–2844.
- [43] A. M. Simon, L. J. Hargrove, B. A. Lock, and T. A. Kuiken, "A Decision-Based Velocity Ramp for Minimizing the Effect of Misclassifications During Real-Time Pattern Recognition Control," *IEEE Trans. Biomed. Eng.*, vol. 58, no. 8, pp. 2360–2368, Aug. 2011.
- [44] T. E. Milner and S. S. Dhaliwal, "Activation of intrinsic and extrinsic finger muscles in relation to the fingertip force vector," *Exp Brain Res*, vol. 146, pp. 197–204, 2002.
- [45] C. E. Lang and M. H. Schieber, "Human Finger Independence: Limitations due to Passive Mechanical Coupling Versus Active Neuromuscular Control," *J. Neurophysiol.*, vol. 92, no. 5, pp. 2802–10, 2004.
- [46] M. H. Schieber and M. Santello, "Hand function: peripheral and central constraints on performance," *J. Appl. Physiol.*, vol. 96, no. 6, pp. 2293–2300, Jun. 2004.
- [47] T. Pistohl, C. Cipriani, A. Jackson, and K. Nazarpour, "Abstract and Proportional Myoelectric Control for Multi-Fingered Hand Prostheses," *Ann. Biomed. Eng.*, vol. 41, no. 12, pp. 2687–2698, Dec. 2013.
- [48] S. M. Radhakrishnan, S. N. Baker, and A. Jackson, "Learning a Novel Myoelectric-Controlled Interface Task," *J. Neurophysiol.*, vol. 100, no. 4, pp. 2397–2408, Oct. 2008.
- [49] J. L. Segil and R. F. F. Weir, "Novel postural control algorithm for control of multifunctional myoelectric prosthetic hands," *J Rehabil Res Dev. J Rehabil Res Dev*, vol. 52, no. 4, pp. 449–466, 2015.
- [50] J. L. Segil, S. A. Huddle, and R. F. F. Weir, "Functional Assessment of a Myoelectric Postural Controller and Multi-Functional Prosthetic Hand by Persons with Trans-Radial Limb Loss," *IEEE Trans. Neural Syst. Rehabil. Eng.*, vol. 25, no. 6, 2017.
- [51] M. Robertus and K. Nazarpour, "Improvements in or relating to Prosthetics," WO2014122455 (A1), 2014.